JACS
JOURNAL OF THE AMERICAN CHEMICAL SOCIETY
Communication
pubs.acs.org/JACS

Direct Characterization of a Reactive Lattice-Confined Ru_2 Nitride by Photocrystallography

Anuvab Das,[†] Joseph H. Reibenspies,[†] Yu-Sheng Chen,[§] and David C. Powers*[,†]

[†]Department of Chemistry, Texas A&M University, College Station, Texas 77843, United States
[§]ChemMatCARS, the University of Chicago, Argonne, Illinois 60439, United States

Supporting Information

ABSTRACT: Reactive metal−ligand (M−L) multiply bonded complexes are ubiquitous intermediates in redox catalysis and have thus been long-standing targets of synthetic chemistry. The intrinsic reactivity of mid-to-late M−L multiply bonded complexes renders these structures challenging to isolate and structurally characterize. Although synthetic tuning of the ancillary ligand field can stabilize M−L multiply bonded complexes and result in isolable complexes, these efforts inevitably attenuate the reactivity of the M−L multiple bond. Here, we report the first direct characterization of a reactive Ru_2 nitride intermediate by photocrystallography. Photogeneration of reactive M−L multiple bonds within crystalline matrices supports direct characterization of these critical intermediates without synthetic derivatization.

Metal−oxygen and metal−nitrogen multiply bonded complexes are critical intermediates in both synthetic and biological oxidation catalysis as well as O_2 and N_2 reduction schemes.[1] As such, complexes featuring metal−ligand (M−L) multiple bonds are longstanding targets for chemical synthesis. High-valent early transition metals support strong M−L multiple bonds via efficient overlap of filled ligand-based π-symmetry orbitals with vacant metal-based π^* orbitals. In contrast, M−L multiple bonds of mid-to-late transition metals, which feature higher d-electron counts and thus destabilizing filled $\pi-\pi^*$ interactions, tend to be reactive.[2] The relative reactivity of mid-to-late M−L multiply bonded complexes renders these structures attractive intermediates for catalysis but challenging species to isolate and structurally characterize. Synthetic tuning of the ancillary ligand field and metal coordination geometry has been pursued extensively to stabilize higher d-electron count M−L multiple bonds;[1a,2] however, the design considerations that allow isolation of these structures inevitably attenuate their reactivity.[3] We are interested in directly characterizing reactive M−L multiple bonds without synthetic derivatization. Here, we report direct crystallographic characterization of a reactive Ru_2 nitride intermediate photogenerated within a crystalline matrix.

Reactive metal nitride complexes are potential intermediates in C−H amination and olefin aziridination reactions.[4] Similar to other reactive M−L multiply bonded complexes, metal nitrides that are sufficiently reactive to functionalize C−H bonds are challenging to structurally characterize because facile oxidative decomposition pathways preclude access to the requisite crystalline samples.[5] The challenges inherent in characterization of reactive metal nitrides are illustrated by the chemistry of Ru_2 nitride **2**, originally reported by Berry and co-workers (Figure 1a).[6] Photolysis of Ru_2 azide complex **1**[7] at low temperature has

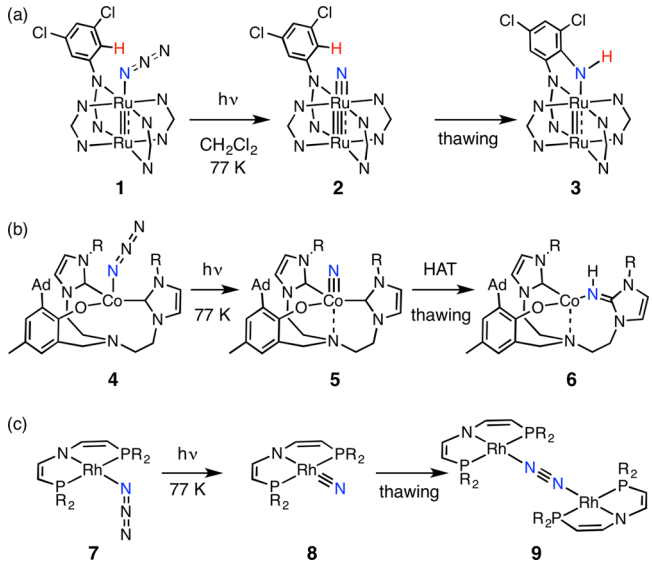

Figure 1. Reactive metal nitrides are challenging to characterize structurally because both intra- (i.e., via amination of pendant C−H bonds (**2** to **3**; N−N: *N*,*N*′-bis(3,5-dichlorophenyl)formamidinate) or *N*-atom insertion into ancillary M−L bonds (**5** to **6**; R: mesityl)) and intermolecular (i.e., nitride dimerization (**8** to **9**; R: *t*-Bu)) decomposition pathways can be facile.

been proposed to generate Ru_2 nitride **2**,[6] which upon warming functionalizes a proximal ligand-based C−H bond to generate Ru_2 amide **3**.[8] Other nitride decomposition pathways, such as insertion into ancillary M−L bonds[9] (i.e., conversion of Co(IV) nitride **5** to Co(II) imine complex **6**,[9a] Figure 1b) and bimolecular nitride coupling reactions[10] to generate N_2 (i.e., conversion of Rh(IV) nitride **8** to N_2-bridged Rh_2 complex **9**,[10a] Figure 1c) are common decomposition pathways of reactive metal nitrides that can preclude crystallization. In the absence of crystallographic data, IR, EPR, electronic absorption spectroscopies and EXAFS spectral fitting have been used, in

Received: December 29, 2016
Published: February 14, 2017

© 2017 American Chemical Society

DOI: 10.1021/jacs.6b13357
J. Am. Chem. Soc. 2017, 139, 2912−2915

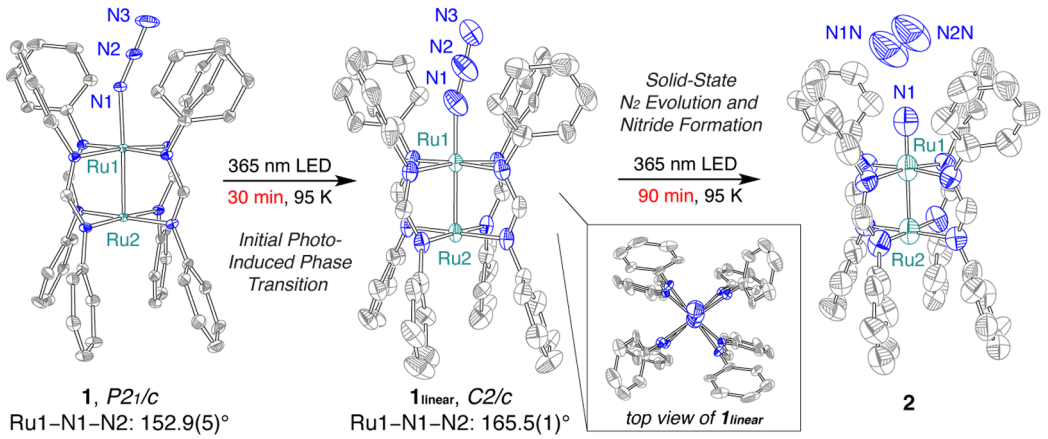

Figure 2. Photocrystallographic characterization of reactive Ru_2 nitride **2**. Photolysis (λ = 365 nm) of a single crystal of Ru_2 azide **1** at 95 K results first in a phase transition ($P2_1/c$ to $C2/c$) to generate $\mathbf{1}_{linear}$, which is promoted by photoinduced crystal heating, and subsequently in extrusion of N_2 to generate Ru_2 nitride complex **2**. Thermal ellipsoids are drawn at 50% probability. H- and Cl-atoms are omitted for clarity. Metrics: **1**, Ru1−Ru2, 2.3445(8) Å; Ru1−N1, 2.047(6) Å; Ru1−N1−N2, 152.9(5)°; $\mathbf{1}_{linear}$, Ru1−Ru2, 2.373(2) Å; Ru1−N1, 2.01(1) Å; Ru1−N1−N2, 165.5(1)°; **2**, Ru1−Ru2, 2.408(3) Å; Ru1−N1, 1.72(2) Å.

combination with high-level calculations, to assign structures for highly reactive M−L multiply bonded intermediates.[11]

We considered that direct structural characterization of highly reactive M−L multiply bonded intermediates could be achieved if the targeted structures could be generated within a crystalline matrix. For example, if a stable molecular precursor of the intermediate of interest could be converted to the reactive species without disrupting the ordered crystal lattice, X-ray diffraction techniques could be utilized to establish the structures of reactive intermediates. Such an experiment is akin to classical matrix isolation experiments. For example, isolation of FeN,[12] RuN, and OsN[13] in both Ar and N_2 matrices has allowed characterization of these reactive fragments by vibrational spectroscopy, but traditional matrix isolation experiments do not allow the structural characterization available in crystalline samples. Coppens and Ohashi have pioneered photocrystallography, an approach for in situ crystallographic characterization of photochemically generated structures.[14] Photocrystallography has been applied to the characterization of organic radicals,[15] carbenes,[16] unsaturated metal complexes,[17] metastable linkage isomers,[18] and molecular excited states.[19] Photocrystallographic experiments are challenging to apply to irreversible photoreactions and have not previously been applied to the characterization of reactive intermediates in C−H functionalization.

We targeted characterization of Ru_2 nitride **2** because (1) in comparison to isolable mononuclear Ru_2 nitride complexes,[20] it has been proposed to exhibit an anomalously long Ru−N bond due to the presence of M−M interactions,[6] (2) it is reactive toward C−H bonds at low temperature,[8] and (3) it has been characterized by EXAFS,[6] which allows benchmarking of our photocrystallographic results. Ru_2 azide **1** crystallizes in a $P2_1/c$ space group and the solid-state absorption spectrum of **1** is well-matched to the solution phase spectrum (Figure S1). A goniometer-mounted crystal of **1** was irradiated with a 365 nm LED source and reaction progress was monitored in real-time by X-ray diffraction at the Advanced Photon Source (APS) housed at Argonne National Laboratory (ANL) (Figure 2). Irradiation of **1** leads initially to a phase transition from a $P2_1/c$ to a $C2/c$ space group. The observed phase transition is accompanied by the linearization of the azide ligand binding mode: the Ru1−N1−N2 bond angle expands from 152.9(5)° to 165.5(1)°. The photoinduced phase transition is not reversible if the light source is removed. Continued irradiation leads to evolution of nitride complex **2**, as evidenced by both the contraction of the Ru1−N1 vector (2.047(6) Å to 1.72(2) Å) and the observation of a new electron density peak above the Ru_2 nitride. The electron density peak integrates as 12 e^- and was satisfactorily modeled as a molecule of N_2 (85% occupancy, see Figure S2 for refinement details). The N_2 molecule is located in a bowl-shaped void space that is defined by the aromatic substituents on the formamidinate ligands.

The metrical parameters of **2** determined by photocrystallography (Ru1−Ru2: 2.408(3) Å; Ru1−N1: 1.72(2) Å) are in good agreement with values extracted from EXAFS spectral fitting (Ru1−Ru2: 2.42 Å; Ru1−N1: 1.76 Å).[6] In addition to bond length information, photocrystallographic structure determination provides direct measurement of bond angles, which are challenging to obtain by other experimental methods. Of note is the linearity of the Ru−Ru−N unit. Comparison of the structure of **2** with a refinement in a triclinic unit cell confirms that the metrical parameters are not symmetry enforced (Table S1).

Ru_2 nitride **2** generated by photolysis of a solid-state powdered-crystalline sample of **1** is spectroscopically identical to **2** generated by photolysis of a frozen CH_2Cl_2 glass of **1**. As shown in Figure 3, photolysis of **1**, as either a powder or as a frozen glass, results in the evolution of an axial EPR signal characteristic of the δ^* ground state of nitride **2**.[6] Powder X-ray diffraction (PXRD) analysis of the solid-state sample confirmed that the powder used in the EPR experiment exhibits the same crystal phase as the sample utilized for photocrystallographic analysis (Figure S3).

As described above, photolysis of Ru_2 azide **1** at 95 K leads first to a $P2_1/c$ to $C2/c$ phase transition that is characterized by linearization of the Ru1−N1−N2 bond angle ($\mathbf{1}_{linear}$), and subsequently to the evolution of nitride **2**. An identical phase transition is observed when photolysis is carried out at 15 K, but at this temperature we do not observe substantial formation of nitride **2**, even after extended photolysis. Because substantial conversion of **1** to **2** was not observed when photolysis was carried out at 15 K, examination of the structural changes

DOI: 10.1021/jacs.6b13357
J. Am. Chem. Soc. 2017, 139, 2912−2915

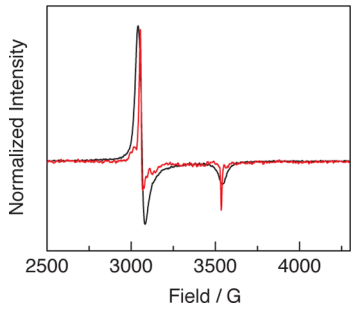

Figure 3. X-band EPR spectra **2** generated in the solid state (powdered crystals, black —) and a frozen CH_2Cl_2 glass (red —) demonstrate that nitride **2** generated in the solid state is spectroscopically indistinguishable from that generated in a frozen glass.

associated with the observed phase transition was pursued with this lower-temperature data set. We considered two possibilities to account for the observed linearization of the azide ligand during photolysis. First, local photoinduced sample heating is common during condensed-phase photoreactions,[21] and thus the observed phase transition could be thermally promoted. Second, we considered that the phase transition may be due to evolution of a thermally trapped molecular excited state.[22]

To explore the origin of the observed phase transition, variable-temperature (VT) X-ray diffraction data for Ru_2 azide **1** were collected between 15 and 250 K; metrical parameters and unit cell data as a function of temperature are presented in Tables S2 and S3. The same $P2_1/c$ to $C2/c$ phase transition that is observed at early irradiation times was observed between 150 and 200 K in the VT crystallography experiment. In addition, the Ru(1)−N(1)−N(2) bond angle is highly temperature dependent, displaying a 150.9(4)° bond angle at 15 K and 168.8(6)° bond angle at 250 K (Figure 4). In contrast, the Ru−Ru distance, which is sensitive to changes in molecular spin state,[23] is invariant with temperature.

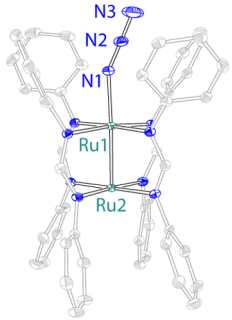

Temp / K	Ru1–N1–N2 / °
15	150.9 (4)
30	151.1 (3)
50	152.1 (4)
95	152.9 (5)
150	156.9 (2)
200	168.7 (5)
250	168.8 (6)
Irradiated at 15 K	165.5 (2)

Figure 4. Temperature dependence of the Ru1−N1−N2 angle in Ru_2 azide **1**. Linearization of this angle upon photolysis at 15 K is consistent with photo-induced heating of the sample.

The size of thermal ellipsoids of atoms that are not involved in the primary photoreaction can be used as an in situ probe of the effective temperature of crystalline samples.[21] Comparison with the thermal ellipsoids of a crystal photolyzed at 15 K with the thermal ellipsoid obtained from VT crystallography reveals that photoinduced heating renders the effective sample temperature closer to 200 K, which is in good agreement with the measured linearization of the azide ligand (data collected in Figure S4). Together, these data suggest that the phase transition that precedes nitride evolution is driven by photoinduced crystal heating. Similar analysis indicates that the effective sample temperature during 95 K irradiation is approximately 350 K (Figure S5; see Supporting Information for additional discussion of sample temperature).

We further confirmed that the phase transition observed crystallographically is not due to a change in electronic structure by photolyzing both solution-phase and powdered samples of **1** in the cavity of an EPR spectrometer maintained at 15 K. No signals were observed other than those attributable to azide **1** and a minor amount of **2** (Figure S6). After photolysis at 15 K, the sample was warmed to 95 K in the dark and no evolution of the EPR spectrum was observed. Taken with the VT X-ray diffraction data, these experiments suggest that photoinduced crystal heating is responsible for the linearization of the azide ligand prior to evolution of nitride **2**.

Attempts to observe conversion of lattice-confined nitride **2** to amido complex **3** were unsuccessful. Consistent with experimentally determined activation parameters,[8] C−H insertion does not proceed at 95 K. Slow warming of crystalline samples of **2** to 200 K led to sample cracking, manifest as diminished diffraction intensity and quality, which precluded observation of C−H functionalization. We speculate that the observed sample cracking may be due to diffusion of lattice-bound N_2 at higher temperature.

The results reported here demonstrate photocrystallography to be a viable approach to investigating directly the structures of highly reactive M−L multiply bonded intermediates relevant to C−H amination. The success of these experiments, which do not require synthetic stabilization of the reactive fragment of interest, are likely due to a combination of low-temperature photogeneration of the targeted reactive intermediates and lattice confinement of those structures, which restricts motions of reactive intermediates. Experimental definition of metrical parameters is critical to rigorous correlation of structure, reactivity, and electronic structure. We anticipate that photocrystallography will contribute to these efforts and may find application as a tool for the direct structure elucidation of additional reactive intermediates.

■ ASSOCIATED CONTENT

Supporting Information

The Supporting Information is available free of charge on the ACS Publications website at DOI: 10.1021/jacs.6b13357.

Experimental procedures and spectroscopic data, VT X-ray diffraction data (PDF)

Data for $C_{52}H_{28}Cl_{16}N_{11}Ru_2$ (CIF)

■ AUTHOR INFORMATION

Corresponding Author

*david.powers@chem.tamu.edu

ORCID

Anuvab Das: 0000-0002-9344-4414

David C. Powers: 0000-0003-3717-2001

Notes

The authors declare no competing financial interest.

■ ACKNOWLEDGMENTS

We thank Greg Wylie for help with EPR measurements, Marcetta Darensbourg for an EPR finger dewar, François Gabbaï for a Xe lamp, as well as Texas A&M University and the Welch Foundation (A-1907) for financial support. ChemMatCARS Sector 15 is principally supported by the NSF under

DOI: 10.1021/jacs.6b13357
J. Am. Chem. Soc. 2017, 139, 2912−2915

grant number NSF/CHE-1346572. Use of the APS was supported by the U.S. DOE under Contract No. DE-AC02-06CH11357.

REFERENCES

(1) (a) Saouma, C. T.; Peters, J. C. *Coord. Chem. Rev.* **2011**, *255*, 920−937. (b) Ortiz de Montellano, P. R. *Chem. Rev.* **2010**, *110*, 932−948. (c) Que, L., Jr. *Acc. Chem. Res.* **2007**, *40*, 493−500. (d) Meunier, B.; de Visser, S. P.; Shaik, S. *Chem. Rev.* **2004**, *104*, 3947−3980. (e) Nugent, W. A.; Mayer, J. M. *Metal Ligand Multiple Bonds*; Wiley & Sons: New York, NY, 1988. (f) Holm, R. H.; Berg, J. M. *Acc. Chem. Res.* **1986**, *19*, 363−370.

(2) (a) Winkler, J. R.; Gray, H. B. *Struct. Bonding* **2011**, *142*, 17−28. (b) Gunay, A.; Theopold, K. H. *Chem. Rev.* **2010**, *110*, 1060−1081. (c) Mayer, J. M. *Comments Inorg. Chem.* **1988**, *8*, 125−135.

(3) Rohde, J.-U.; In, J. H.; Lim, M. H.; Brennessel, W. W.; Bukowski, M. R.; Stubna, A.; Munck, E.; Nam, W.; Que, L., Jr. *Science* **2003**, *299*, 1037−1039.

(4) (a) Smith, J. M. *Prog. Inorg. Chem.* **2014**, *58*, 417−470. (b) Berry, J. F. *Comments Inorg. Chem.* **2009**, *30*, 28−66. (c) Eikey, R. A.; Abu-Omar, M. M. *Coord. Chem. Rev.* **2003**, *243*, 83−124.

(5) (a) Atienza, C. C. H.; Bowman, A. C.; Lobkovsky, E.; Chirik, P. J. *J. Am. Chem. Soc.* **2010**, *132*, 16343−16345. (b) Knobloch, D. J.; Lobkovsky, E.; Chirik, P. J. *Nat. Chem.* **2010**, *2*, 30−35. (c) Schöffel, J.; Šušnjar, N.; Nückel, S.; Sieh, D.; Burger, P. *Eur. J. Inorg. Chem.* **2010**, *2010*, 4911−4915. (d) Schlangen, M.; Neugebauer, J.; Reiher, M.; Schröder, D.; López, J. P.; Haryono, M.; Heinemann, F. W.; Grohmann, A.; Schwarz, H. *J. Am. Chem. Soc.* **2008**, *130*, 4285−4294.

(6) Pap, J. S.; DeBeer George, S.; Berry, J. F. *Angew. Chem., Int. Ed.* **2008**, *47*, 10102−10105.

(7) Chen, W.-Z.; De Silva, V.; Lin, C.; Abellard, J.; Marcus, D. M.; Ren, T. *J. Cluster Sci.* **2005**, *16*, 151−165.

(8) (a) Long, A. K. M.; Timmer, G. H.; Pap, J. S.; Snyder, J. L.; Yu, R. P.; Berry, J. F. *J. Am. Chem. Soc.* **2011**, *133*, 13138−13150. (b) Long, A. K. M.; Yu, R. P.; Timmer, G. H.; Berry, J. F. *J. Am. Chem. Soc.* **2010**, *132*, 12228−12230.

(9) (a) Zolnhofer, E. M.; Käß, M.; Khusniyarov, M. M.; Heinemann, F. W.; Maron, L.; van Gastel, M.; Bill, E.; Meyer, K. *J. Am. Chem. Soc.* **2014**, *136*, 15072−15078. (b) Buschhorn, D.; Pink, M.; Fan, H.; Caulton, K. G. *Inorg. Chem.* **2008**, *47*, 5129−5135. (c) Ingleson, M. J.; Pink, M.; Fan, H.; Caulton, K. G. *J. Am. Chem. Soc.* **2008**, *130*, 4262−4276.

(10) (a) Scheibel, M. G.; Wu, Y.; Stückl, A. C.; Krause, L.; Carl, E.; Stalke, D.; deBruin, B.; Schneider, S. *J. Am. Chem. Soc.* **2013**, *135*, 17719−17722. (b) Scheibel, M. G.; Askevold, B.; Heinemann, F. W.; Reijerse, E. J.; de Bruin, B.; Schneider, S. *Nat. Chem.* **2012**, *4*, 552−558. (c) Betley, T. A.; Peters, J. C. *J. Am. Chem. Soc.* **2004**, *126*, 6252−6254.

(11) Rohde, J.-U.; Betley, T. A.; Jackson, T. A.; Saouma, C. T.; Peters, J. C.; Que, L., Jr. *Inorg. Chem.* **2007**, *46*, 5720−5726.

(12) Andrews, L.; Citra, A.; Chertihin, G. V.; Bare, W. D.; Neurock, M. *J. Phys. Chem. A* **1998**, *102*, 2561−2571.

(13) Citra, A.; Andrews, L. *J. Phys. Chem. A* **2000**, *104*, 1152−1161.

(14) (a) Kawano, M. *Bull. Chem. Soc. Jpn.* **2014**, *87*, 577−592. (b) Cole, J. M. *Chem. Soc. Rev.* **2004**, *33*, 501−513.

(15) (a) Kawano, M.; Sano, T.; Abe, J.; Ohashi, Y. *J. Am. Chem. Soc.* **1999**, *121*, 8106−8107. (b) Abe, J.; Sano, T.; Kawano, M.; Ohashi, Y.; Matsushita, M.; Iyoda, T. *Angew. Chem., Int. Ed.* **2001**, *40*, 580−582.

(16) (a) Kawano, M.; Hirai, K.; Tomioka, H.; Ohashi, Y. *J. Am. Chem. Soc.* **2001**, *123*, 6904−6908. (b) Kawano, M.; Hirai, K.; Tomioka, H.; Ohashi, Y. *J. Am. Chem. Soc.* **2007**, *129*, 2383−2391.

(17) Kawano, M.; Kobayashi, Y.; Ozeki, T.; Fujita, M. *J. Am. Chem. Soc.* **2006**, *128*, 6558−6559.

(18) (a) Carducci, M. D.; Pressprich, M. R.; Coppens, P. *J. Am. Chem. Soc.* **1997**, *119*, 2669−2678. (b) Kawano, M.; Ishikawa, A.; Morioka, Y.; Tomizawa, H.; Miki, E.; Ohashi, Y. *J. Chem. Soc., Dalton Trans.* **2000**, 2425−2431. (c) Bowes, K. F.; Cole, J. M.; Husheer, S. L. G.; Raithby, P. R.; Savarese, T. L.; Sparkes, H. A.; Teat, S. J.; Warren, J. E. *Chem. Commun.* **2006**, 2448−2450. (d) Warren, M. R.; Brayshaw, S. K.; Johnson, A. L.; Schiffers, S.; Raithby, P. R.; Easun, T. L.; George, M. W.; Warren, J. E.; Teat, S. J. *Angew. Chem., Int. Ed.* **2009**, *48*, 5711−5714.

(19) (a) Novozhilova, I. V.; Volkov, A. V.; Coppens, P. *J. Am. Chem. Soc.* **2003**, *125*, 1079−1087. (b) Ozawa, Y.; Terashima, M.; Mitsumi, M.; Toriumi, K.; Yasuda, N.; Uekusa, H.; Ohashi, Y. *Chem. Lett.* **2003**, *32*, 62−63.

(20) For examples, see: (a) Walstrom, A.; Pink, M.; Yang, X.; Tomaszewski, J.; Baik, M.-H.; Caulton, K. G. *J. Am. Chem. Soc.* **2005**, *127*, 5330−5331. (b) Man, W.-L.; Tang, T.-M.; Wong, T.-W.; Lau, T.-C.; Peng, S.-M.; Wong, W.-T. *J. Am. Chem. Soc.* **2004**, *126*, 478−479.

(21) Schmøkel, M. S.; Kamiński, R.; Benedict, J. B.; Coppens, P. *Acta Crystallogr., Sect. A: Found. Crystallogr.* **2010**, *66*, 632−636.

(22) Svendsen, H.; Overgaard, J.; Chevallier, M.; Collet, E.; Iversen, B. B. *Angew. Chem., Int. Ed.* **2009**, *48*, 2780−2783.

(23) Angaridis, P.; Cotton, F. A.; Murillo, C. A.; Villagrán, D.; Wang, X. *J. Am. Chem. Soc.* **2005**, *127*, 5008−5009.

DOI: 10.1021/jacs.6b13357
J. Am. Chem. Soc. 2017, 139, 2912−2915